Myopathy mutations in α-skeletal-muscle actin cause a range of molecular defects

Céline F. Costa[1,*], Heidi Rommelaere[2], Davy Waterschoot[2], Kamaljit K. Sethi[1], Kristen J. Nowak[3,4,‡], Nigel G. Laing[3,4], Christophe Ampe[2] and Laura M. Machesky[1,§]

[1]School of Biosciences, Division of Molecular Cell Biology, University of Birmingham, Birmingham B15 2TT, UK
[2]Department of Biochemistry, Ghent University and Flanders Interuniversity Institute for Biotechnology (VIB09), B-9052 Gent, Belgium
[3]Centre for Neuromuscular and Neurological Disorders, University of Western Australia, Australian Neuromuscular Research Institute, Nedlands, and [4]Centre for Medical Research, West Australian Institute for Medical Research, QEII Medical Centre, Nedlands, WA 6009, Australia
*Present address: Department of Pathology, CMU, University of Geneva, 1211 Geneva 4, Switzerland
‡Present address: Department of Human Anatomy and Genetics, University of Oxford, South Parks Road, Oxford OX1 3QX, UK
§Author for correspondence (e-mail: l.m.machesky@bham.ac.uk)

Accepted 23 February 2004
Journal of Cell Science 117, 3367-3377 Published by The Company of Biologists 2004
doi:10.1242/jcs.01172

Summary

Mutations in the gene encoding α-skeletal-muscle actin, *ACTA1*, cause congenital myopathies of various phenotypes that have been studied since their discovery in 1999. Although much is now known about the clinical aspects of myopathies resulting from over 60 different *ACTA1* mutations, we have very little evidence for how mutations alter the behavior of the actin protein and thus lead to disease. We used a combination of biochemical and cell biological analysis to classify 19 myopathy mutants and found a range of defects in the actin. Using in vitro expression systems, we probed actin folding and actin's capacity to interact with actin-binding proteins and polymerization. Only two mutants failed to fold; these represent recessive alleles, causing severe myopathy, indicating that patients produce nonfunctional actin. Four other mutants bound tightly to cyclase-associated protein, indicating a possible instability in the nucleotide-binding pocket, and formed rods and aggregates in cells. Eleven mutants showed defects in the ability to co-polymerize with wild-type actin. Some of these could incorporate into normal actin structures in NIH 3T3 fibroblasts, but two of the three tested also formed aggregates. Four mutants showed no defect in vitro but two of these formed aggregates in cells, indicating functional defects that we have not yet tested for. Overall, we found a range of defects and behaviors of the mutants in vitro and in cultured cells, paralleling the complexity of actin-based muscle myopathy phenotypes.

Key words: Actin, Nemaline myopathy, Actin polymerization, Protein folding, Myopathy, Actin mutations

Introduction

Congenital myopathies resulting from mutations in the gene encoding α-skeletal-muscle actin, *ACTA1*, show various phenotypes that have been divided into three classes based on the morphology observed in patient muscle biopsies (Sparrow et al., 2003). These myopathies have a range of severity, from mild (with long-term survival and only minor muscle weakness), to severe (with lethality shortly after birth). The three classes are: actin myopathy (AM), which is characterized by an excess of thin filamentous inclusions located in what would normally be the myofibrillar filament lattice; intranuclear-rod myopathy (IRM); and nemaline myopathy (NEM), which is characterized by sarcoplasmic deposits containing actin and actin-binding proteins (ABPs) termed 'nemaline bodies' (Sparrow et al., 2003). Although NEM is the most common form of congenital myopathy caused by actin mutations, many patients show more than one histological phenotype in their muscle biopsies, such as the combination of nemaline bodies and intranuclear rods or excess thin filaments. However, Sparrow et al. were able to classify some of the categories of congenital myopathies based on clustering of mutations on the three-dimensional (3D) structure of actin. They could then make predictions about which functional defects in actin might be present in patients with a certain mutation and phenotype (Sparrow et al., 2003).

Newly synthesized actin is processed in a special folding pathway to become functionally active. The nascent actin is transferred, by the chaperone prefoldin, from the ribosome to the cytosolic chaperonin (CCT), which assists actin in its folding in an ATP-dependent manner and releases it as an active folded monomer (Gao et al., 1992; Vainberg et al., 1998). Once actin is properly folded, it assumes the form of a monomer and polymerizes into a filament. The proportion of monomer actin in cells depends mainly on the regulation by actin-binding proteins. In skeletal muscle, most of the actin is filamentous and is the main component of the thin filament. Other thin filament proteins can also be mutated in congenital myopathies, including α-tropomyosin (*TPM3*) (Laing et al., 1995), β-tropomyosin (*TPM2*) (Donner et al., 2002), troponin T1 (*TNNT1*) (Johnston et al., 2000) and nebulin (*NEB*) (Pelin et al., 1999). For a recent review, see Wagner (Wagner, 2002).

Mutations in *ACTA1* are suggested to account for 20% of NEM cases (Sparrow et al., 2003). Studies of actin NEM and AM have provided extensive clinical descriptions of cases and the precise mutations involved (Ryan et al., 2003; Sparrow et

al., 2003). To gain insight into the molecular mechanisms of actin myopathies, we selected 19 different myopathy mutations for biochemical and in vitro cell analysis. Our studies reveal that the different actin mutations result in a range of functional defects, which correlate with predictions made by reference to the 3D actin structure but do not correlate with the severity of the disease. Our findings agree with a report from Ryan et al. (Ryan et al., 2003) that the clinical course correlates poorly with the muscle pathology in NEM. They also provided the first insights into the spectrum of defects that occur in the actin molecule and lead to a range of features in patient muscles.

Mutants showed various levels of impaired function, which we divided into four categories. The most defective mutants were trapped on the chaperone proteins CCT and prefoldin, indicating that they did not fold properly (category I). The next most severe defects (category II) showed an increased affinity for the cyclase-associated protein (CAP), which has a high affinity for the nucleotide-free state of actin and can indicate folding instability (Rommelaere et al., 2003). CAP binds in the subdomain 1-3 cleft of the actin monomer (Rommelaere et al., 2003) and acts with cofilin to promote rapid actin turnover in mammalian cells (Moriyama and Yahara, 2002). It has connections with Ras signaling in yeast and is proposed to sequester actin monomers in *Dictyostelium*, but very little is known about its function in mammals (Freeman and Field, 2000; Gerst et al., 1991; Noegel et al., 2003). Most of the actin mutants folded, bound normally to DNase I, Vitamin-D-binding protein (DBP), thymosin-β4 and profilin (categories III and IV), but category III mutants showed reduced ability to co-polymerize with wild-type actin.

By expressing several of the actin mutants in an in vitro cell culture system, we found, in seven out of ten cases, a correlation between whether patients had nemaline bodies and similar deposits of actin in the cultured cells. Overall, we propose that actin-based congenital myopathies occur via several molecular mechanisms, ranging from an unstable actin monomer to more subtle changes in molecular interactions or function.

Materials and Methods

Construction of the α-actin NEM mutants

ACTA1 mutations were made with the Quick Change site directed mutagenesis kit (Stratagene, UK) according to the manufacturer's instructions, using the *ACTA1* cDNA sequence in pcDNA3.1 (Invitrogen, UK) as a template and appropriate primers. N-Terminal Myc-tagged wild-type and actin mutants were made by the polymerase chain reaction using the actin mutants in the pcDNA3.1 vector as template, a 5′ primer containing the Myc sequence preceded by a *Hin*dIII site and a 3′ primer containing an *Xba*I site. These fragments were ligated into *Hin*dIII- and *Xba*I-digested pcDNA3.1. Constructs were sequenced to verify the complete *ACTA1* coding sequence and correct introduction of the desired mutation.

Expression of actin mutants and band-shift assays with ABPs

We expressed α-skeletal-muscle actins (wild-type and mutants) as ^{35}S-labeled proteins by in vitro transcription translation reactions in reticulocyte lysate (Promega, UK) according to the manufacturer's instructions, using 0.02 μCi ^{35}S-methionine (MP Biochemicals) and 200 ng DNA per 25 μl reaction. After incubation at 30°C for 1.5 hours, we analysed the reaction products on denaturing tricine gels (Schagger and von Jagow, 1987) and on non-denaturing polyacrylamide gels according to Safer (Safer, 1989) with ATP, followed by autoradiography. To monitor CAP binding, ATP was omitted from the gels. CAP is present as an endogenous protein in the reticulocyte lysates and has been previously identified on native gels under these conditions (Rommelaere et al., 2003). The amount of ^{35}S-actin bound to CAP was quantified by phosphor imaging (Typhoon 9200 variable mode imager; Amersham Biosciences) and the Image Quant software package. For the band-shift assays, 1 μl of a solution of each ABP (DNase I, DBP, profilin-IIA or thymosin-β4) was added to 3 μl of the in vitro transcription translation reaction. After a 1 minute incubation, the mixture was analysed on native gels containing 200 μM ATP. The final concentration of the actin binding proteins was 8 μM for DNase I, 4.8 μM for DBP, 12.5 μM for thymosin-β4 and 60 μM for profilin-IIA. These concentrations are the minimal amounts of the ABPs needed to cause a band shift of wild-type actin, as determined by a concentration series (data not shown) (Rommelaere et al., 2003). We note that relatively weak interactions (i.e. thymosin β4 mutants have a K_d of 100 μM) can be monitored using this assay (Van Troys et al., 1996). Binding capacity was inspected by eye. Reduced binding means that only a part of the population of the mutant actin molecules shifted, and part remained unshifted (Rommelaere et al., 2003). DNase I was purchased from Worthington and DBP from Calbiochem. Thymosin-β4 was chemically synthesized on a model 431A peptide synthesizer using solid phase FMOC chemistry. Recombinant profilin-IIA was purified according to Lambrechts et al. (Lambrechts et al., 2000).

Co-polymerization assays

25 μl of an in vitro transcription translation reaction of wild-type or mutant α-skeletal-muscle actin was centrifuged at 450,000 ***g*** in a Beckman airfuge to remove aggregates. To the supernatant, we added 25 μl of 12 μM actin, purified from rabbit skeletal muscle according to Pardee and Spudich (Pardee and Spudich, 1982) in G buffer (2 mM Tris-HCl, pH 8, 0.2 mM $CaCl_2$, 0.5 mM DTT, 0.2 mM ATP); that is, approximately a 500-fold excess of wild-type actin over mutant (or in vitro translated control wild-type) actin. Polymerization was induced for 2 hours at room temperature, by adding KCl and $MgCl_2$ to a final concentration of 100 mM and 1 mM, respectively (F buffer). F-Actin was pelleted by centrifugation at 450,000 ***g*** for 20 minutes. The supernatant was removed (supernatant 1), the pellet washed and resuspended in 80 μl G buffer for an overnight depolymerization at 4°C. A second round of polymerization was induced for 2 hours. F-Actin was again centrifuged at 450,000 ***g*** for 20 minutes, and supernatant 2 was removed from the final pellet. Aggregates, supernatants 1 and 2, and the final pellet were analysed on a 12.5% sodium dodecyl sulfate (SDS) gel followed by autoradiography. The amount of ^{35}S-labeled actin in each fraction was quantified using phosphor imaging. All mutants were analysed at least three times.

Cell culture and transfection

NIH 3T3 fibroblasts were cultured at 37°C in humidified 5% CO_2 atmosphere. They were maintained in a proliferation medium composed of Dulbecco's modified Eagle's medium (DMEM) supplemented with 5% donor calf serum (Gibco BRL, UK), 1% penicillin/streptomycin and 20 mM L-glutamine (Gibco BRL, UK). We transfected pcDNA3.1 vectors encoding N-terminally Myc-tagged α-skeletal-muscle actin (wild type or mutant) using Lipofectamine 2000 transfection reagent (Gibco BRL, UK) according to the manufacturer's protocol.

Immunofluorescence and microscopy

Cells were plated on glass coverslips (prewashed with nitric acid). At given times, they were washed three times in PBS and fixed with 4% formaldehyde for 10 minutes at room temperature. Free aldehyde

groups were blocked with 50 mM NH_4Cl for 10 minutes and cells were permeabilized with PBS with 0.1% Triton X-100 for 4 minutes. Cells were incubated with anti-Myc antibody (Cancer Research UK) for 40 minutes at room temperature followed by a Texas-red anti-mouse secondary antibody (Jackson ImmunoResearch) and FITC-phalloidin (Sigma, UK) for 40 minutes. All antibodies were diluted in PBS with 1% bovine serum albumin. Finally, coverslips were rinsed three times in water and mounted onto a slide with 5 μl Mowiol (Calbiochem) plus Antifade. In some cases additional Hoechst staining was applied (0.4 μg ml^{-1}) (Hoechst 33342, Sigma). Stained cells were examined with a Zeiss microscope (Zeiss, Jena, Germany) using a 63× objective. Images were recorded with a Hammamatsu C4880 camera (Bridgewater, NJ) and processed using Openlab software (Improvision, Lexington, MA).

Results

The 19 mutations (encompassing 17 residues) that we selected for this study are located throughout the four subdomains of the actin molecule and lead to different severities of disease. They are displayed in green on the 3D representation of the molecule (Fig. 1). One of the residues, G15, directly contacts the β-phosphate of the adenine nucleotide (Kabsch et al., 1990), G182 is in the nucleotide-binding pocket and R183 has been implicated in closure of the nucleotide cleft. The other mutations are scattered throughout the molecule. Some are near binding sites for ABP or intersubunit contacts in the filament (Table 1, Fig. 1). In muscles, they induce different abnormal structures such as intranuclear and cytoplasmic rods and/or an excess of thin filaments (Table 1). Recently, Rommelaere et al. (Rommelaere et al., 2003) have performed an alanine scan of the whole β-actin molecule. They found that the location of particular alanine mutations on the actin molecule can induce different defects, including deficiency in folding, loss of binding to ABP or polymerization defects. In addition, extensive studies of yeast actin have used alanine-scanning mutagenesis of surface residues to analyse genetic interactions, and revealed key binding sites of ABPs as well as functional residues (Ayscough and Drubin, 1996).

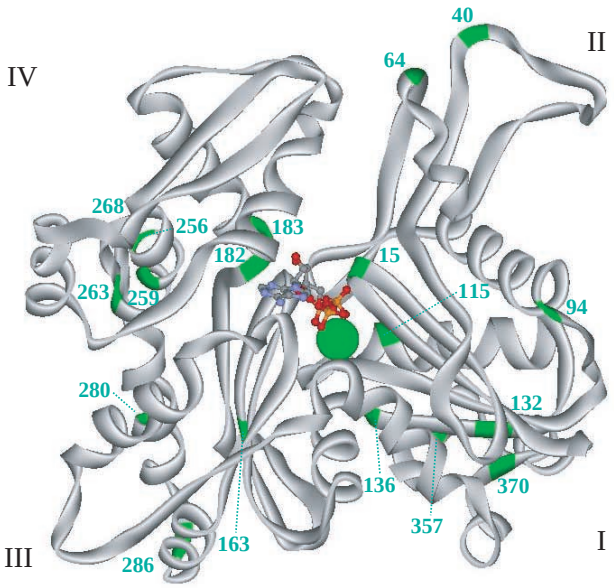

Fig. 1. Location of *ACTA1* mutations on the three-dimensional representation of the actin molecule. The 19 mutations selected for this study, encompassing 17 residues, are located on the four subdomains of the actin molecule (labeled I-IV). They lead to different severities of disease. The structure was taken from PDB code 1ATN and displayed by NetViewerLite (Accessory Software).

Table 1. The congenital myopathy mutations investigated in this study

Mutation	Phenotype	Lethality¶	Type of mutation	Position or function in actin structure*,†	ABP prediction
G15R	AM	3 months	De novo	ATP-binding	
H40Y	Severe, NEM, IRM	2 months	De novo	F-Actin contact, hydrophobic pocket	Myosin, DNase I, thymosin β4*
I64N	Typical, NEM	Alive 8 years, 48 years	Dominant	F-Actin contact, hydrophobic pocket	DNase I*
L94P	Severe, NEM	5 days, 19 days with G259V	Recessive	Buried	
N115S	Typical, NEM	Alive 33 years, 18 years, 3 years	Dominant	Buried, near nucleotide cleft	α-Actinin
M132V	Mild, NEM	Alive 39 years, 9 years	?	Buried	
I136M	Mild, NEM	Alive 45 years	?	Hinge region	
V163L	AM, IRM	Alive 5 months, 4 months	De novo	Buried, near nucleotide cleft	CAP‡
G182D	Typical, NEM	Alive 3 years	De novo	In nucleotide cleft	CAP‡
R183C	Severe, NEM	1 day, 4 days	Dominant	Hydrogen bonds for nucleotide cleft closure	
R183G	Typical/severe, NEM	13 months, 1 year	De novo	Hydrogen bonds for nucleotide cleft closure	Tropomodulin§
G259V	Severe, NEM	5 days, 19 days with L94P	Recessive	Buried	
Q263L	Severe, NEM	Alive 21 months	Dominant	Surface, near hydrophobic plug	
G268C	Mild/typical NEM	Alive 10 years, 7 years	De novo	F-Actin contact, hydrophobic pocket	
G268R	Severe, NEM	Alive 5 years	?	F-Actin contact, hydrophobic pocket	
N280K	Severe, NEM	9 months	De novo	Surface near F-actin contact	DBP
D286G	Severe, NEM	9 months	De novo	F-actin contact along the strands and hydrophobic pocket	Profilin
I357L	Severe, NEM, IRM	6 months	De novo	?	α-Actinin, nebulin, tropomyosin
V370F	Severe, NEM	Alive 4 months	De novo	?	α-Actinin, tropomyosin, DBP, myosin

The mutations selected for this study induce different phenotypes and symptoms in patients. All data were taken from Sparrow et al. (Sparrow et al., 2003), which summarizes data from other articles (Nowak et al., 1999; Ilkovski et al., 2001), with the exception of those marked as follows: *Kabsch et al., 1990; †Holmes et al., 1990; ‡Rommelaere et al., 2003; §Krieger et al., 2002. ¶Where more than one age is given, this refers to multiple patients.

Abbreviations: AM, actin myopathy, excess of thin filaments; CAP, cyclase-associated protein; DBP, vitamin-D-binding protein; IRM, intranuclear rod myopathy; NEM, nemaline myopathy, sarcoplasmic nemaline bodies.

Some mutants have a folding defect and/or structural instability

The initial requirement for function of actin is proper folding (Gao et al., 1992; Vainberg et al., 1998), and so we first investigated which *ACTA1* myopathy mutants could fold correctly. For this assay, and also for the other in vitro experiments, we expressed 19 *ACTA1* mutants in reticulocyte lysates, which endogenously contain CAP (McCormack et al., 2002) and the actin folding machinery: prefoldin and CCT (Gao et al., 1992; Rommelaere et al., 1993; Vainberg et al., 1998). The ^{35}S-labeled products were analysed on native polyacrylamide gels. Proteins that do not fold properly stick to CCT and prefoldin. We also tested whether these mutants could associate with various actin-monomer-binding proteins (thymosin-β4, DBP, profilin-IIa and DNase I) to indicate further whether they were correctly folded (Rommelaere et al., 2003).

Of the 19 mutants tested, 16 migrated at a position similar to monomeric actin (Fig. 2), two were not released from CCT and prefoldin (L94P and E259V; Fig. 2), and one (G182D) was released but remained bound to CAP even in the presence of ATP (Fig. 2A). Although less L94P and E259V appear to be produced than of the other mutants (Fig. 2), we observed that, on SDS gels, the signals from these mutants were roughly the same as for the other mutants (not shown), so we attribute this decrease in signal to unfolded protein migrating aberrantly on native gels or failing to enter at all. L94P showed marginal association with DBP and with DNase I, whereas none of the ABPs shifted E259V (Fig. 3), further indicating highly defective proteins.

Mutants that have aberrant nucleotide binding are thought to form a tight complex with CAP (Rommelaere et al., 2003). For G182D, 60% of total mutant protein associated with CAP (Fig. 2), suggesting that it has impaired nucleotide binding. However, this mutant shifted on native gels with other ABPs, indicating correct folding (Fig. 3). Three other mutants, G15R, N115S and V163L, can fold, indicated by some protein migrating on the gel position of monomeric actin (Fig. 2) but associate more with CAP in the absence of ATP than wild-type actin does (12%, 6% and 8%, respectively, compared with 2% for wild-type); in addition, V163L associates more with CCT (21%) and prefoldin (8%) than does wild-type actin (9% with CCT and 3% with prefoldin) (Fig. 2). This indicates that some mutants might be less stable than the wild type in structure and in nucleotide binding, and that V163L might also be partially impaired in folding. However, these three mutants, and the other 13 that were released from CCT, were able to shift when the ABPs were added, indicating that they were capable of reaching a correctly folded state and were sufficiently stable to form some interactions. DNase I only partially shifted I64N (Fig. 3), which might be due to the location of residue 64 in the major contact site between DNase I and actin (Kabsch et al., 1990).

Some mutants have a co-polymerization defect

Myopathy mutations might alter actin polymerization, so we tested whether the mutants could co-polymerize with wild-type actin. We expressed ^{35}S-labeled mutants and induced them to co-polymerize with wild-type rabbit α-skeletal-muscle actin (Fig. 4). Mutant actin incorporation into filaments was measured by quantifying ^{35}S levels either in the initial spin (aggregates) before adding carrier actin and inducing polymerization or in the supernatant (G-actin) of the two high-speed spins following polymerization, or in the final pellet (F-actin). Wild-type actin polymerized to about 60% in this assay and was used as a standard. Several mutants polymerized to at least 50% and were considered to be similar to wild-type actin, within the error margins of our assay (H40Y, M132V, V163L, R183C and D286G). Most of the mutants (H40Y, M132V, R183C and D286G) also bound to the ABP tested and were thus classified as 'category IV' with no observable defect in

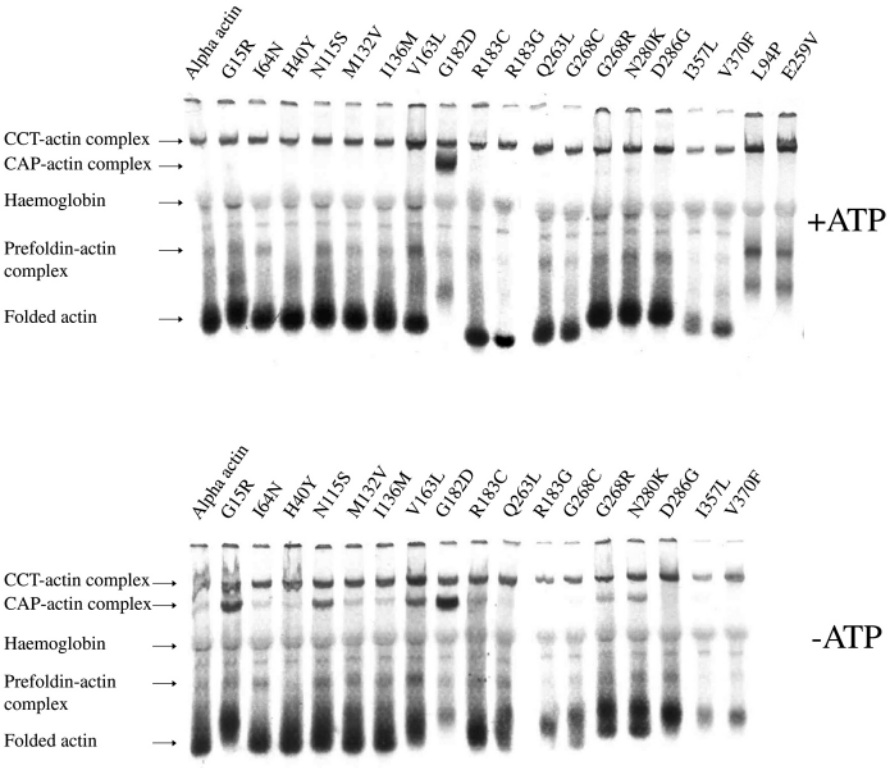

Fig. 2. Behavior of actin mutants on native gels. The ^{35}S-labeled products of the in vitro translation assays were run on native polyacrylamide gels with or without ATP and imaged using autoradiography. On the native gel with ATP, G182D stuck to CAP and both mutants L94P and E259V remained bound to CCT and prefoldin, and showed an absence of folded actin. The 16 other mutants were folded correctly, as indicated by an abundance of folded actin that was similar to the wild type. On the gel without ATP, G15R, N115S, V163L and G182D showed an increase in binding to CAP. Representative gels shown from three experiments performed.

our assays. V163L was classed as category II, because it showed increased CAP binding, although it could co-polymerize with wild-type actin. This mutant also formed significantly more aggregates in the co-polymerization assay than the wild-type actin (Fig. 4, $P<0.01$ from Student's *t*-test), which is consistent with it being less stable. The mutant G15R was borderline, polymerizing to about 40%. Because it also showed increased CAP binding, it was also included in category II. Several mutants had more severely reduced co-polymerization capacity compared with wild-type actin, mostly polymerizing to less than 25% (I64N, N115S, I136M, G182D, R183G, Q263L, G268C, G268R, N280K, I357L, V370F). From these, the mutants that did not show increased CAP binding were singled out as having a polymerization defect and classified as category III (I64N, I136M, R183G, Q263L, G268C, G268R, N280K, I357L, V370F). N280K might also have formed more aggregates than the wild-type actin, although this result was not significant in Student's *t*-test (Fig. 4).

In addition to defects in co-polymerization, mutants could have poisoning activities against polymerization (such as capping one end of a filament) or even enhanced polymerization ability, given that some patients have excess thin filaments (Goebel et al., 1997). We did not observe any gross change in the total amount of F-actin in our assays, which would have been expected if one of these activities were present, but this kind of defect was not likely to be picked up given the high concentrations of wild-type actin required in the assay.

Mutant actins give a variety of phenotypes in fibroblasts

We did not express the non-folding mutants from category I but we did express representative mutants from categories II, III and IV in NIH3T3 fibroblasts to examine their ability to participate in actin dynamics in cells. We also expressed some mutants that induce intranuclear rods in patients (Table 1) to test whether they formed similar structures in cultured cells. Our initial studies were with C2C12 or H2K myoblast cell lines but we found that the exogenous expression of even wild-type actin was detrimental to these cells (data not shown), making it impossible to study mutant actin expression in them in enough detail to report here. We therefore chose a fibroblast model, NIH3T3, that is relatively easy to transfect and that tolerates exogenous actin expression well, but with the obvious caveat that we will only observe general causes of dysregulation of the actin system. We found that wild-type actin with an N-terminal Myc tag was incorporated into stress fibers and lamellipodia (Fig. 5A). All structures that stained with phalloidin in these cells also showed co-staining with anti-Myc antibody (Fig. 5A-A″), indicating a good incorporation into cellular F-actin pools of the exogenous muscle actin. Muscle actin has previously been shown in several studies to incorporate well into fibroblast cytoskeletons (Machesky and Hall, 1997; Mounier et al., 1999; Theriot and Mitchison, 1992). Subtle differences are likely to occur owing to the different

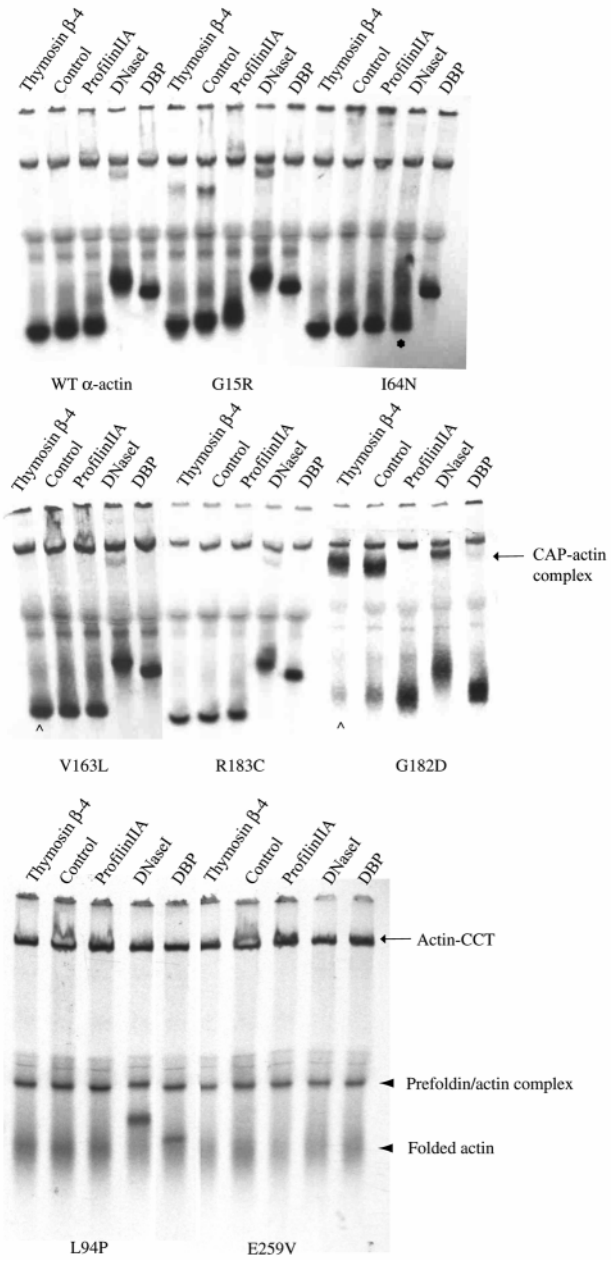

Fig. 3. Interaction between α-skeletal-muscle actin and the different mutants with thymosin β4, profilin-IIA, DNase I and vitamin-D-binding protein (DBP). ^{35}S-Labeled α-skeletal-muscle actin and mutants were produced by in vitro translation, run on native gels after mixing with thymosin β4, profilin IIa, DNase I or DBP and subjected to autoradiography. Wild-type α-skeletal-muscle actin shifted up (profilin, DNase I, DBP) or down (thymosin β4) in complex with ABPs compared with α-skeletal-muscle actin alone. Most of the mutants interacted with the different ABPs (Table 2). R183C and G15R are shown as examples of those that behaved like the wild type; the others are not shown but are listed in Table 2. The control lanes in each case represent the mutant actin run in the absence of added ABP. The mutant I64N was only partially shifted when DNAse I was added (asterisk). The mutants L94P and E259V remained associated with CCT (arrow) and prefoldin and the released product (arrowhead) showed little (L94P) or no (E259V) binding to ABPs. The mutants G182D and V163L, which stuck to CAP, did not shift with thymosin β4 (up arrow), which might reflect the relatively low affinity of actin for thymosin and competition with CAP. Both mutants shifted with DBP and DNase I, however, indicating proper folding. The gel shown is a representative of three experiments with similar results.

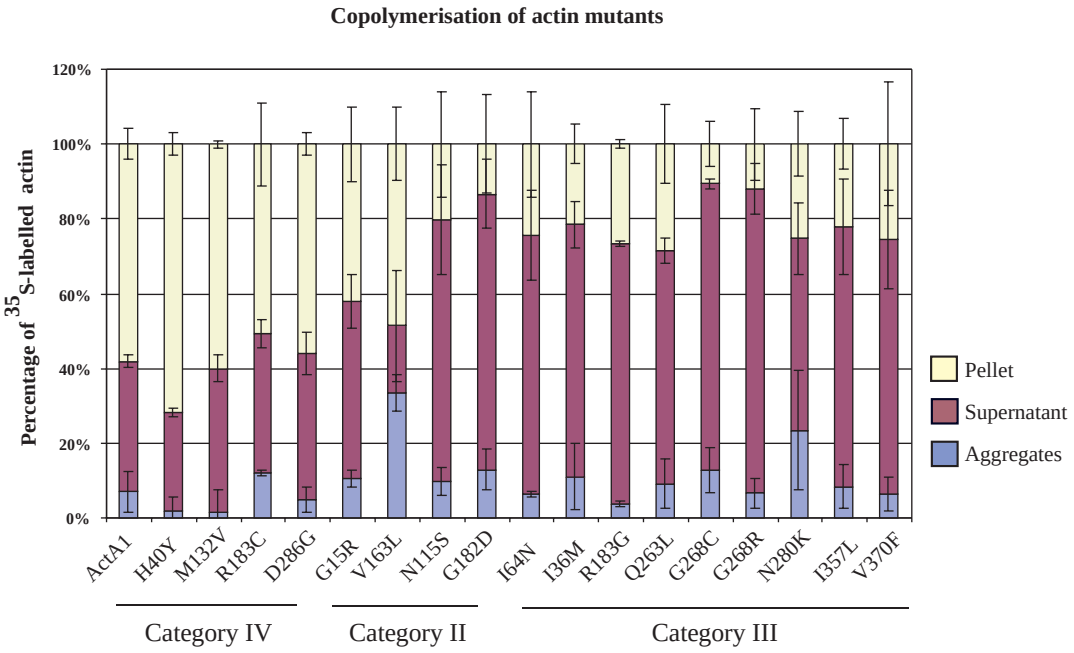

Fig. 4. Co-polymerization assays of wild type α-skeletal-muscle actin and mutants. Samples of an in vitro transcription-translation reaction and α-actin from rabbit skeletal muscle were mixed, induced to polymerize and pelleted. The amounts of ^{35}S-labeled actin in aggregates (first pellet, before polymerization and without carrier actin), supernatants (did not pellet under any conditions) and final pellets (F-actin, after two rounds of polymerization) were calculated. Mutants with more than 50% of the ^{35}S-labeled actin in filaments were considered to be 'wild type'. These include H40Y, M132V, V163L, R183C and D286G. G15R had only 40% polymerization and was considered to be 'borderline'. Mutants with less than 50% of ^{35}S-labeled actin in filaments were considered to be impaired in co-polymerization: I64N, N115S, I136M, G182D, R183G, Q263L, G268C, G268R, N280K, I357L, V370F.

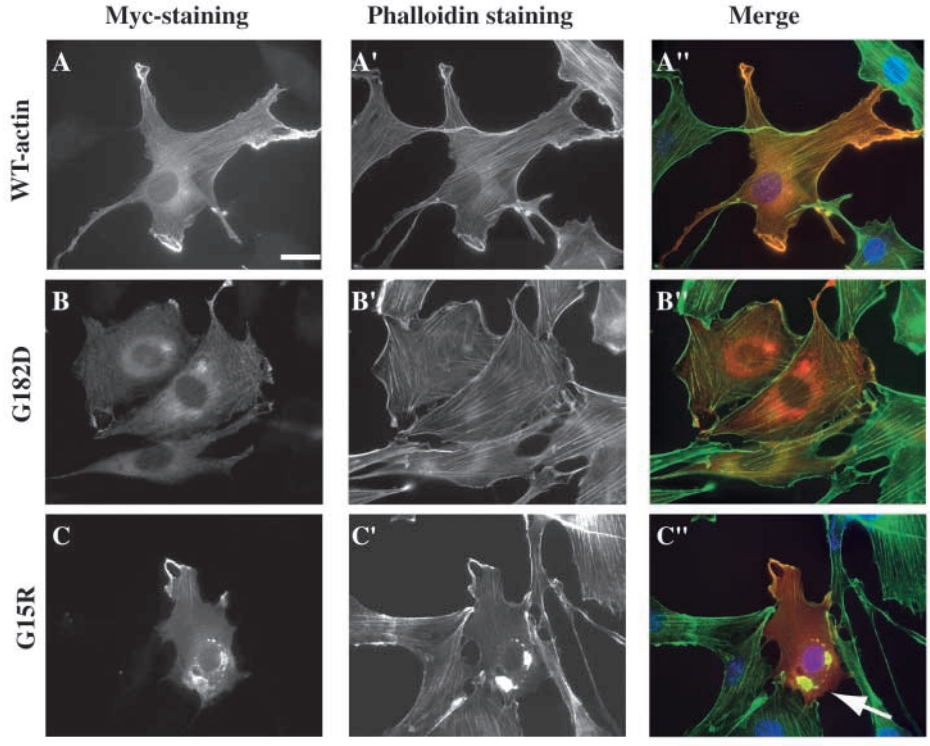

Fig. 5. Expression of wild-type and category-II (CAP-associated) mutants in NIH3T3 fibroblasts. Wild-type actin (A; scale bar, 25 μm) was transfected as a control and was incorporated into stress fibers, ruffles and lamellipodia, and generally co-localized with the endogenous filamentous actin, as visualized with phalloidin (A′,A″). The mutant G182D showed a dotted pattern in the cytoplasm (B) and co-localized with the endogenous actin in stress fibers and lamellipodia (B′,B″). G15R was partially incorporated into the stress fibers and lamellipodia (C). In some cells, the mutant protein formed aggregates that stained with phalloidin (C,C″, arrow). (A″-C″) Red corresponds to the Myc staining and green to the phalloidin staining. (A″,C″) Nuclei were stained with Hoechst and appear blue.

actin isoforms having slightly different properties in vivo (Mounier and Sparrow, 1997). However, we were assaying for gross morphological structures (stress fibers, ruffles, aggregates, rods).

From category II, we expressed G182D and G15R, which showed increased CAP binding (60% and 12%, respectively) and a modest reduction in co-polymerization. G182D localized weakly to stress fibers and lamellipodia, and also in a punctate pattern to the cytoplasm, with some actin clouds around the nucleus (Fig. 5B-B″). G15R was incorporated into stress fibers and filamentous actin in lamellipodia (Fig. 5C-C″) but also formed aggregates that stained with phalloidin (Fig. 5C-C″).

Overall, the category III mutants that we expressed behaved largely like wild-type actin in NIH3T3 cells. Mutants I136M

and G268R co-localized with stress fibers and actin in lamellipodia (data not shown). However, I64N localized to small aggregates and long rods in the cytoplasm in addition to normal actin structures (Fig. 6A, arrow). These rods did not stain with phalloidin (Fig. 6A, arrow), indicating that they were not composed of filamentous actin or were not accessible to phalloidin.

As representatives of category IV mutants, which behaved roughly like the wild-type actin in all of our in vitro assays, we expressed mutants M132V and D286G. M132V incorporated in stress fibers and filamentous actin in lamellipodia and appeared similar to wild-type actin (not shown). The mutant D286G, however, either incorporated into abnormal wavy stress fibers (Fig. 6B, inset) or formed aggregates in the cytoplasm and the nucleus that did not stain with phalloidin (Fig. 6C).

V163L (category II), I357L (category III) and H40Y (category IV) showed intranuclear rods in patient biopsies, so we investigated whether these mutants behaved similarly in cultured cells. Both V163L and H40Y formed intranuclear rods in NIH3T3 cells (Fig. 7A-C) in addition to other aberrant actin cytoskeleton structures. Neither mutant incorporated into stress fibers or other endogenous normal actin structures. All of the aberrant structures stained with phalloidin, suggesting that they were composed of filaments. V163L additionally induced aggregation of endogenous actin, because some aggregates were detectable with phalloidin staining only (Fig. 7B arrows). H40Y was also incorporated in clouds, aggregates and little rods in random locations in the cytoplasm that stain with phalloidin (Fig. 7C and not shown). I357L incorporated into normal actin structures and also formed small punctate cytoplasmic aggregates that did not stain with phalloidin (Fig. 7D). Thus, we saw rods and/or aggregates in all three mutants tested, although none were intranuclear for I357L.

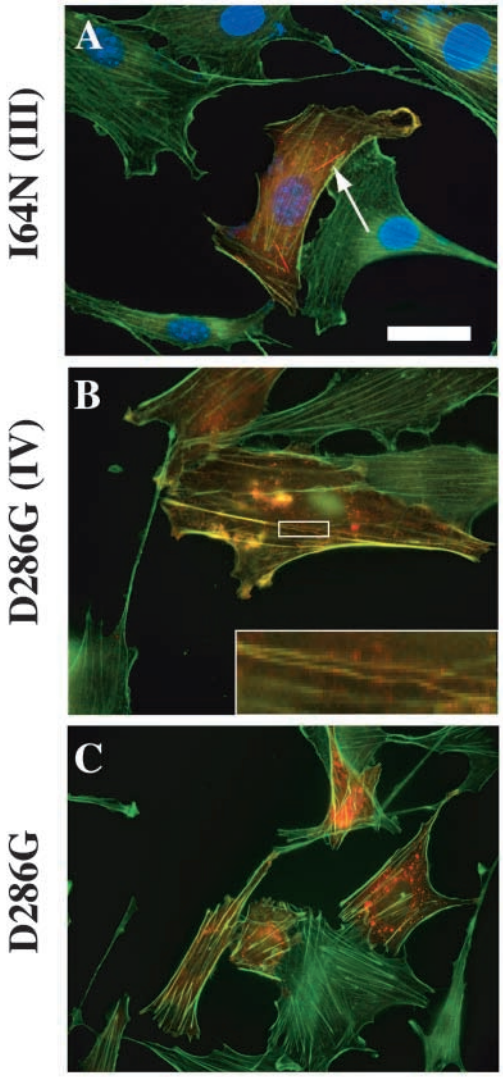

Fig. 6. Expression of category III (co-polymerization defect) and category IV (no biochemical defect) mutants in NIH3T3 fibroblasts. I64N incorporated into stress fibers, localized with the endogenous actin and was observed in aggregates and long rods in the cytoplasm, which did not stain with phalloidin (A; scale bar, 25 μm). D286G incorporated into stress fibers in some cells (B) but their structures were wavy (B, inset). D286G also formed aggregates in the cytoplasm that did not stain with phalloidin (C). (A-C) Red indicates Myc staining and green phalloidin staining. (A) The nuclei were stained with Hoechst and appear blue.

Discussion

To our knowledge, this study provides the first experimental evidence of molecular defects in actin caused by different *ACTA1* mutations that result in human muscle disease. From the in vitro results, we classified the mutants into various categories of severity, ranging from folding/stability defects to wild-type behavior in all assays. Thus, the range of patient phenotypes in myopathy caused by actin mutations is probably due to the different behaviors of the mutants. However, the severity of the molecular defects does not necessarily correlate with the severity of the disease. Disease is probably caused by 'poisonous' actin that prevents the endogenous actin from having normal cellular dynamics (polymerization, ABP binding and sarcomere contraction/integrity). Dosage of actin expression is unlikely to be a problem, because adult heterozygote-null patients are normal (Sparrow et al., 2003). Nemaline bodies might or might not be important in the disease process, because their effect on cellular function is not known and their presence and abundance do not obviously correlate with the severity of the disease (Ryan et al., 2003).

Category I: non-folding mutants are recessive and cause severe myopathy

Mutants L94P and E259V are especially interesting clinically, because they are the only examples of recessive mis-sense mutations identified to date. If the two mutant genes are inherited together (one from each parent), they produce offspring with severe NEM from apparently normal heterozygous parents. Sparrow et al. predicted that L94P and E259V might be totally non-functional actin mutants that were benign when mixed with the wild type. We found that neither of these mutants could fold properly or release from CCT or prefoldin. This also indicates that the folding machinery can cope with at least one folding-defective copy of actin, which we found to be surprising given the abundance of actin and the possibility of excess unfolded protein jamming the folding machinery.

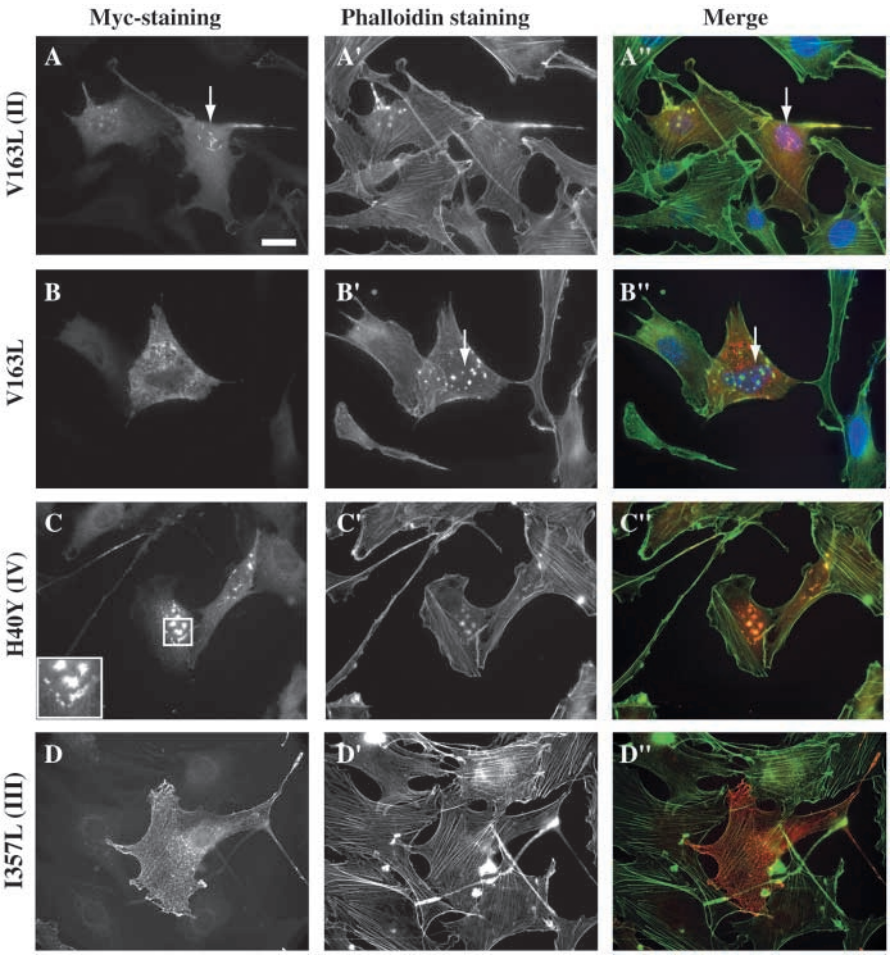

Fig. 7. Rod formation by expression of V163L (category II), H40Y (category IV) and I357L (category III) in NIH3T3 fibroblasts. V163L did not localize to normal actin structures but recruited endogenous actin to aberrant structures (A-A″,B-B″, arrows). In the nucleus, it formed aggregate star structures (A-A″; scale bar, 25 μm). Some aggregates were stained with phalloidin but did not detectably contain the mutant actin (B-B″ arrows). H40Y did not localize to normal actin structures but formed rods and aggregates in the nucleus and cytoplasm (C-C″ and not shown). I357L (D-D″) incorporated into stress fibers and lamellipodia and also formed cytoplasmic aggregates, which did not localize with endogenous actin. (A′-D′) Red indicates Myc staining and green phalloidin staining. The nuclei were stained with Hoechst and appear blue.

Category II: actins that show increased CAP binding have mutations in or near actin's nucleotide-binding cleft

Mutants G15R, N115S, V163L, G182D, reside at or near the nucleotide-binding cleft and were predicted to affect nucleotide binding (Sparrow et al., 2003). We found that these bound tightly to CAP on native gels (either with or without ATP), as also observed for nucleotide-free actin (Rommelaere et al., 2003). G15 takes part in a β-hairpin whose backbone makes direct contact with the β-phosphate of the nucleotide (Kabsch et al., 1990). Introduction of an arginine might disrupt the structure of this β-hairpin, resulting in loss of nucleotide binding. N115, V163 and G182 do not directly contact the nucleotide but the mutations might alter the local structures so that the nucleotide binding is prevented, especially by introducing a negative charge at position 182. The increased CAP binding might indicate that these mutants are unstable, which might lead to some of the aggregate structures observed in NEM, IRM and AM, and by expression of G15R, V163L and G182D in fibroblasts.

Category III: mutants with a co-polymerization defect

About half of the mutations causing a co-polymerization defect are located at or near the polymer contacts in actin filaments. In the F-actin model proposed by Holmes et al. (Holmes et al., 1990), actin protomers are associated in two strings wound around each other in a right-handed helix, with interactions along and across the strands. The interactions between molecules along one strand involve contacts between subdomain 4 and subdomain 2 of one protomer with subdomain 3 of the next (i.e. residues 243-245 contact residues 322-325, residues 202-204 contact residues 286-289 and residues 41-45 contact residues 166-169 and 375). Contacts across the two strands are made between subdomain-1 residues 110-112 of one protomer and residues 195-197 in subdomain 4 of the other, and by the so-called hydrophobic plug (residues 266-269), which inserts into a hydrophobic pocket formed by residues 166, 169, 171, 173, 285, 289 and residues 40-45,63 and 64 of two adjacent protomers in one strand (Holmes et al., 1990). Eight of the NEM mutations are at (H40Y, I64N, G268C, G268R and D286G) or near (V163L, Q263L, N280K) polymer contacts and these were predicted to cause polymerization defects (except for N280K and V163L) (Sparrow et al., 2003). Five of these mutants (I64N, Q263L, G268C, G268R and N280K) had a lower co-polymerization capacity than the wild type but H40Y, V163L and D286G polymerized similarly to the wild type. Thus, location at or near the polymer contact was a good predictor of a polymerization defect, but was not 100% accurate, indicating the need for experimental testing of predictions based on structure.

Some analogs of category-III mutants have been studied in other systems, giving potentially additional insight into the defect that might occur in myopathy patients. The hydrophobic plug mutation G268R, which incorporated into normal actin structures in NIH3T3 despite reduced co-polymerization capacity, is an example of one of these. When G268D was expressed homozygously in the indirect flight muscle of *Drosophila melanogaster*, it induced wavy fibers but the heterozygote was normal (An and Mogami, 1996). L267D in yeast actin resulted in a mild phenotype (a cold-sensitive polymerization defect) (Chen et al., 1993). In addition, the

Table 2. Summary of the complete study

	Folding	Binding to ABPs	Polymerization	In NIH fibroblasts	Severity
Category I: folding defect					
L94P	No	No	Not done	Not done	Severe NEM
E259V	No	No	Not done	Not done	Severe NEM
Category II: fold, binds to CAP					
G15R	Stays on CAP without ATP	Yes	WT	SF, small cytoplasmic rods, cytoplasmic aggregates	AM
N115S	Stays on CAP without ATP	Yes	<WT	Not done	Mild and typical NEM
V163L	Stays on CAP without ATP	Yes	WT	Nuclear and cytoplasmic aggregates, IR no SF	AM, IRM
G182D	Stays on CAP with/ without ATP	Not thymosin β4	<WT	SF, actin dots	Typical NEM
Category III: copolymerisation defect					
I64N	Yes	Partially to DNaseI	<WT	SF, cytoplasmic aggregates and rods	Typical NEM
I136M	Yes	Yes	<WT	SF	Typical NEM
G268C	Yes	Yes	<WT	Not done	Mild NEM
R183G/Q263L N280K/V370F	Yes	Yes	<WT	Not done	Severe NEM
G268R	Yes	Yes	<WT	SF	Severe NEM
I357L	Yes	Yes	<WT	SF, actin dots	Severe NEM, IRM
Category IV: no defect in vitro					
H40Y	Yes	Yes	WT	Nuclear and cytoplasm aggregates, IR no SF	Severe NEM, IRM
M132V	Yes	Yes	<WT	SF	Mild NEM
R183C	Yes	Yes	<WT	Not done	Severe NEM
D286G	Yes	Yes	<WT	Aggregates and abnormal SF	Severe NEM

Results obtained in vitro and in cell expression are summarized, as well as the patient phenotypes per category of defect.
AM, actin myopathy-excess thin filaments; IR, intranuclear rods; IRM, IR myopathy; NEM, nemaline myopathy; SF, stress fibers; WT, same as the wild type; <WT, less than the wild type.

polymerization defect of the yeast actin double mutant V266G/L267G was restored by overexpression of wild-type actin (Kuang and Rubenstein, 1997). It thus appears that actin mutated near or at residue 268 has partial functional capacity and can participate in F-actin structures in cells, but probably causes the formation of less stable actin structures by changing the conformation of the plug or its motion. In vivo, filament-stabilizing proteins might somewhat alleviate these instabilities.

Surprisingly, six other mutations that conferred reduced co-polymerization lie completely outside the polymer contacts (N115S, I136M, G182D, R183G, I357L and V370F). However, N115S and G182D probably have altered ATP binding, whereas I136M and R183G might have altered ADP-ATP exchange, which could affect structural stability and polymer formation. I136M is predicted to disrupt the hinge region between the two actin domains, which will interfere with nucleotide-cleft opening and closure necessary for the ADP-ATP exchange. Similarly, R183G might disrupt the hydrogen bonds with S14 and E71 necessary to maintain closure of the nucleotide-binding pocket. Additionally, R183G might prevent tropomodulin from binding at the pointed end of the actin helix (Krieger et al., 2002), because the hydrophobic plug and α-helix 182-195 are involved in the binding of tropomodulin, which regulates the length of filaments in muscle (Littlefield et al., 2001). The binding defect might explain the severity of the disease caused by this mutation and would be consistent with the abnormal sarcomeres observed in rat cardiomyocytes when mutated tropomodulin was expressed (Sussman et al., 1998). Further investigations of the interaction of R183C/G mutants with tropomodulin might lead to a fuller understanding of this mutation. Likewise, I357L, N115S and V370F might be impaired in α-actinin binding (McGough et al., 1994) and thus disrupt the order of the sarcomere. A previous study found that expression of truncated α-actinin in myoblasts disrupted normal cross-linking of the thin filaments and induced the formation of aggregates and nemaline bodies. In later stage myotubes, it induced hypertrophied Z-bands and nemaline bodies composed of α-actinin and actin, whereas, in PtK2 cells, it induced the breakdown of the stress fibers into clumps containing α-actinin and actin (Schultheiss et al., 1992).

Category IV: mutants that behaved like wild-type in biochemical assays

The mutants H40Y, M132V, R183C and D286G grouped in category IV and did not have any defect in vitro. We assume that the mutations are likely to interfere with interactions with other ABP, such as myosin II or components of the thin filament (Table 1). They might also cause polymerization or actin-dynamics defects that were too subtle to be detected in our assays, because H40Y and D286G showed abnormal structures when expressed in cultured cells (see below). M132V was associated with a mild phenotype in two separate patients (Jungbluth et al., 2001; Sparrow et al., 2003) and

behaved similarly to wild-type actin in cells, so its effect might be subtle, muscle-cell specific or be a result of long-term expression.

Recreation of aggregates and rods observed in muscle cells in a fibroblast model

We investigated the cellular behavior of ten mutants that provoked nemaline bodies in either the sarcoplasm or the nucleus of patients. Seven of these induced aggregates and rods in fibroblasts (G15R, H40Y, I64N, V163L, G182D, D286G, I357L; Table 2). The overall different environments between NIH3T3 cells and muscle tissue, and the timescale of our experiments versus human development might explain why the other four mutants behaved differently in cells than in patients. We found no correlation between the category of mutant and whether patient tissues showed rods (Table 2). This might not be surprising, because some patients with identical mutations show different clinical phenotypes, whether AM, IRM, NEM or a combination of these (Table 1, examples V163L, I357L and H40Y).

Patient samples from V163L, I357L and H40Y show intranuclear rods with an appearance of parallel bundles of filaments (Goebel and Warlo, 1997; Ilkovski et al., 2001; Nowak et al., 1999). It is not clear why these patients have nuclear rods in addition to the generally observed cytoplasmic rods in NEM. In our hands, I357L formed cytoplasmic aggregates, in contrast to H40Y and V163L, which formed rods and star-shaped structures in the nuclei of fibroblasts. The nuclear rods stained with phalloidin, indicating filamentous actin, and this correlates with the fact that these mutants co-polymerize apparently normally in vitro. The function and form of actin in the nucleus remains a subject of debate but it is well known that, under various conditions (including heat shock and DMSO addition to cells), actin can accumulate in the nucleus in rods and aggregates, and might be paracrystalline in form (Iida et al., 1992; Ono et al., 1996). Actin has a nuclear export signal (residues 170-181 and 211-222) (Wada et al., 1998), which allows its transport out of the nucleus; thus, if any of the mutations affected export, this could lead to accumulation. However, none of the mutations causing intranuclear rods in patients are located in these regions, suggesting that the nuclear export was affected by an indirect mechanism.

Rods and aggregates induced by I357, I64N and V163L did not stain with phalloidin, whereas the ones induced by H40Y, V163L, G15R, G182D and D286G did, indicating that different types of aggregates can form. It is not known whether nemaline bodies in patient samples stain with phalloidin. Based on our expression studies, we predict that it will be possible to recreate the aggregate, intranuclear and cytoplasmic rod phenotypes observed in patients in a tissue culture model. We hope that this will provide a platform for further investigation of molecular mechanisms for myopathy phenotypes.

Conclusions

Our results indicate that actin mutations in myopathy do not cause one common defect of actin but rather affect various functions, and although, in many cases, structural predictions are a good indicator of the likely molecular defects of actin (Sparrow et al., 2003), there will in some cases be significant differences. Most of the mutant actins folded properly, were released from CCT and prefoldin, and bound to the tested actin-monomer-binding proteins, but roughly half of them appeared to be impaired in polymerization. Some of the mutants might be unstable, as indicated by increased binding to CAP, which might lead to some of the aggregate structures observed in NEM, IRM and AM. Most tagged mutant actins expressed in cultured fibroblasts produced rods and aggregates similar to those observed in patients. Overall, the combination of in vitro translation of mutants and expression of tagged mutants in cell culture has allowed us to characterize some of the molecular defects associated with myopathies caused by *ACTA1* mutations. We hope that our assays will be useful for future studies of *ACTA1*-based myopathies and will lead to a clearer picture of the causes and potential treatments for congenital actin myopathies.

This work was supported by Muscular Dystrophy Campaign grant RA3/583/3 to L.M.M. and by an MRC senior research fellowship to L.M.M. C.F.C. is supported by a Scientific Projects Committee studentship of the University of Birmingham. H.R. has been a Postdoctoral Fellow of The Fund for Scientific Research – Flanders (FWO-Vlaanderen) and is now supported by the Flanders Interuniversity Institute for Biotechnology (VIB). This work was supported by grants FWO-G.0136.02 (to C.A. and H.R.) and GOA 12051401 of the Concerted Research Actions of the Flemish Community to Joël Vandekerckhove and C.A. N.G.L. and K.J.N. are supported by the Australian National Health and Medical Research Council – Fellowship Grant 139170 and C. J. Martin Fellowship 212086, respectively.

References

An, H. S. and Mogami, K. (1996). Isolation of 88F actin mutants of *Drosophila melanogaster* and possible alterations in the mutant actin structures. *J. Mol. Biol*. **260**, 492-505.

Ayscough, K. R. and Drubin, D. G. (1996). Actin: general principles from studies in yeast. *Annu. Rev. Cell Dev. Biol*. **12**, 129-160.

Chen, X., Cook, R. K. and Rubenstein, P. A. (1993). Yeast actin with a mutation in the 'hydrophobic plug' between subdomains 3 and 4 (L266D) displays a cold-sensitive polymerization defect. *J. Cell. Biol.* **123**, 1185-1195.

Donner, K., Ollikainen, M., Ridanpaa, M., Christen, H. J., Goebel, H. H., de Visser, M., Pelin, K. and Wallgren-Pettersson, C. (2002). Mutations in the beta-tropomyosin (*tpm2*) gene – a rare cause of nemaline myopathy. *Neuromuscular Disord*. **12**, 151-158.

Freeman, N. L. and Field, J. (2000). Mammalian homolog of the yeast cyclase associated protein, CAP/Srv2p, regulates actin filament assembly. *Cell Motil. Cytoskeleton* **45**, 106-120.

Gao, Y., Thomas, J. O., Chow, R. L., Lee, G. H. and Cowan, N. J. (1992). A cytoplasmic chaperonin that catalyzes beta-actin folding. *Cell* **69**, 1043-1050.

Gerst, J. E., Ferguson, K., Vojtek, A., Wigler, M. and Field, J. (1991). CAP is a bifunctional component of the *Saccharomyces cerevisiae* adenylyl cyclase complex. *Mol. Cell. Biol*. **11**, 1248-1257.

Goebel, H. H. and Warlo, I. (1997). Nemaline myopathy with intranuclear rods – intranuclear rod myopathy. *Neuromuscular Disord*. **7**, 13-19.

Goebel, H. H., Anderson, J. R., Hubner, C., Oexle, K. and Warlo, I. (1997). Congenital myopathy with excess of thin myofilaments. *Neuromuscular Disord.* **7**, 160-168.

Holmes, K. C., Popp, D., Gebhard, W. and Kabsch, W. (1990). Atomic model of the actin filament. *Nature* **347**, 44-49.

Iida, K., Matsumoto, S. and Yahara, I. (1992). The KKRKK sequence is involved in heat shock-induced nuclear translocation of the 18-kDa actin-binding protein, cofilin. *Cell Struct. Funct*. **17**, 39-46.

Ilkovski, B., Cooper, S. T., Nowak, K., Ryan, M. M., Yang, N., Schnell, C., Durling, H. J., Roddick, L. G., Wilkinson, I., Kornberg, A. J. et al. (2001). Nemaline myopathy caused by mutations in the muscle alpha-skeletal-actin gene. *Am. J. Hum. Genet*. **68**, 1333-1343.

Johnston, J. J., Kelley, R. I., Crawford, T. O., Morton, D. H., Agarwala, R., Koch, T., Schaffer, A. A., Francomano, C. A. and Biesecker, L. G. (2000). A novel nemaline myopathy in the Amish caused by a mutation in troponin t1. *Am. J. Hum. Genet.* **67**, 814-821.

Jungbluth, H., Sewry, C. A., Brown, S. C., Nowak, K. J., Laing, N. G., Wallgren-Pettersson, C., Pelin, K., Manzur, A. Y., Mercuri, E., Dubowitz, V. et al. (2001). Mild phenotype of nemaline myopathy with sleep hypoventilation due to a mutation in the skeletal muscle alpha-actin (*ACTA1*) gene. *Neuromuscular Disord.* **11**, 35-40.

Kabsch, W., Mannherz, H. G., Suck, D., Pai, E. F. and Holmes, K. C. (1990). Atomic structure of the actin:DNase-I complex. *Nature* **347**, 37-44.

Krieger, I., Kostyukova, A., Yamashita, A., Nitanai, Y. and Maeda, Y. (2002). Crystal structure of the C-terminal half of tropomodulin and structural basis of actin filament pointed-end capping. *Biophys. J.* **83**, 2716-2725.

Kuang, B. and Rubenstein, P. A. (1997). Beryllium fluoride and phalloidin restore polymerizability of a mutant yeast actin (V266G, L267G) with severely decreased hydrophobicity in a subdomain 3/4 loop. *J. Biol. Chem.* **272**, 1237-1247.

Laing, N. G., Wilton, S. D., Akkari, P. A., Dorosz, S., Boundy, K., Kneebone, C., Blumbergs, P., White, S., Watkins, H., Love, D. R. et al. (1995). A mutation in the alpha tropomyosin gene TPM3 associated with autosomal dominant nemaline myopathy. *Nat. Genet.* **9**, 75-79. [Erratum in *Nat. Genet.* (1995). **10**, 249.]

Lambrechts, A., Braun, A., Jonckheere, V., Aszodi, A., Lanier, L. M., Robbens, J., van Colen, I., Vandekerckhove, J., Fassler, R. and Ampe, C. (2000). Profilin II is alternatively spliced, resulting in profilin isoforms that are differentially expressed and have distinct biochemical properties. *Mol. Cell. Biol.* **20**, 8209-8219.

Littlefield, R., Almenar-Queralt, A. and Fowler, V. M. (2001). Actin dynamics at pointed ends regulates thin filament length in striated muscle. *Nat. Cell. Biol.* **3**, 544-551.

Machesky, L. M. and Hall, A. (1997). Role of actin polymerization and adhesion to extracellular matrix in Rac- and Rho-induced cytoskeletal reorganization. *J. Cell Biol.* **138**, 913-926.

McCormack, E. A., Rohman, M. J. and Willison, K. R. (2001). Mutational screen identifies critical amino acid residues of beta-actin mediating interaction between its folding intermediates and eukaryotic cytosolic chaperonin CCT. *J. Struct. Biol.* **135**, 185-197.

McGough, A., Way, M. and DeRosier, D. (1994). Determination of the alpha-actinin-binding site on actin filaments by cryoelectron microscopy and image analysis. *J. Cell Biol.* **126**, 433-443.

Moriyama, K. and Yahara, I. (2002). Human CAP1 is a key factor in the recycling of cofilin and actin for rapid actin turnover. *J. Cell Sci.* **115**, 1591-1601.

Mounier, N., Desmouliere, A. and Gabbiani, G. (1999). Subcutaneous tissue fibroblasts transfected with muscle and nonmuscle actins: a good in vitro model to study fibroblastic cell plasticity. *Wound Repair Regen.* **7**, 45-52.

Mounier, N. and Sparrow, J. C. (1997). Structural comparisons of muscle and nonmuscle actins give insights into the evolution of their functional differences. *J. Mol. Evol.* **44**, 89-97.

Noegel, A. A., Blau-Wasser, R., Sultana, H., Muller, R., Israel, L., Schleicher, M., Patel, H. and Weijer, C. J. (2003). The cyclase associated protein cap as regulator of cell polarity and camp signaling in *Dictyostelium*. *Mol. Biol. Cell* **15**, 934-945.

Nowak, K. J., Wattanasirichaigoon, D., Goebel, H. H., Wilce, M., Pelin, K., Donner, K., Jacob, R. L., Hubner, C., Oexle, K., Anderson, J. R. et al. (1999). Mutations in the skeletal muscle alpha-actin gene in patients with actin myopathy and nemaline myopathy. *Nat. Genet.* **23**, 208-212.

Ono, S., Abe, H. and Obinata, T. (1996). Stimulus-dependent disorganization of actin filaments induced by overexpression of cofilin in c2 myoblasts. *Cell Struct. Funct.* **21**, 491-499.

Pardee, J. D. and Spudich, J. A. (1982). Purification of muscle actin. *Methods Enzymol.* **85**, 164-181.

Pelin, K., Hilpela, P., Donner, K., Sewry, C., Akkari, P. A., Wilton, S. D., Wattanasirichaigoon, D., Bang, M. L., Centner, T., Hanefeld, F. et al. (1999). Mutations in the nebulin gene associated with autosomal recessive nemaline myopathy. *Proc. Natl. Acad. Sci. USA* **96**, 2305-2310.

Rommelaere, H., van Troys, M., Gao, Y., Melki, R., Cowan, N. J., Vandekerckhove, J. and Ampe, C. (1993). Eukaryotic cytosolic chaperonin contains t-complex polypeptide 1 and seven related subunits. *Proc. Natl. Acad. Sci. USA* **90**, 11975-11979.

Rommelaere, H., Waterschoot, D., Neirynck, K., Vandekerckhove, J. and Ampe, C. (2003). Structural plasticity of functional actin: pictures of actin binding protein and polymer interfaces. *Structure* **11**, 1279-1289.

Ryan, M. M., Ilkovski, B., Strickland, C. D., Schnell, C., Sanoudou, D., Midgett, C., Houston, R., Muirhead, D., Dennett, X., Shield, L. K. et al. (2003). Clinical course correlates poorly with muscle pathology in nemaline myopathy. *Neurology* **60**, 665-673.

Safer, D. (1989). An electrophoretic procedure for detecting proteins that bind actin monomers. *Anal. Biochem.* **178**, 32-37.

Schagger, H. and von Jagow, G. (1987). Tricine-sodium dodecyl sulfate-polyacrylamide gel electrophoresis for the separation of proteins in the range from 1 to 100 kDa. *Anal. Biochem.* **166**, 368-379.

Schultheiss, T., Choi, J., Lin, Z. X., DiLullo, C., Cohen-Gould, L., Fischman, D. and Holtzer, H. (1992). A sarcomeric alpha-actinin truncated at the carboxyl end induces the breakdown of stress fibers in ptk2 cells and the formation of nemaline-like bodies and breakdown of myofibrils in myotubes. *Proc. Natl. Acad. Sci. USA* **89**, 9282-9286.

Sparrow, J. C., Nowak, K. J., Hayley, J. D., Beggs, A. H., Walgren-Pettersson, C., Romero, N., Nonaka, I. and Laing, N. G. (2003). Muscle disease caused by mutations in the skeletal muscle alpha-actin gene (*ACTA1*). *Neuromuscular Disord.* **13**, 519-531.

Sussman, M. A., Baque, S., Uhm, C. S., Daniels, M. P., Price, R. L., Simpson, D., Terracio, L. and Kedes, L. (1998). Altered expression of tropomodulin in cardiomyocytes disrupts the sarcomeric structure of myofibrils. *Circ. Res.* **82**, 94-105.

Theriot, J. A. and Mitchison, T. J. (1992). Comparison of actin and cell surface dynamics in motile fibroblasts. *J. Cell Biol.* **119**, 367-377.

Vainberg, I. E., Lewis, S. A., Rommelaere, H., Ampe, C., Vandekerckhove, J., Klein, H. L. and Cowan, N. J. (1998). Prefoldin, a chaperone that delivers unfolded proteins to cytosolic chaperonin. *Cell* **93**, 863-873.

Van Troys, M., Dewitte, D., Goethals, M., Carlier, M. F., Vandekerckhove, J. and Ampe, C. (1996). The actin binding site of thymosin beta 4 mapped by mutational analysis. *EMBO J.* **15**, 201-210.

Wada, A., Fukuda, M., Mishima, M. and Nishida, E. (1998). Nuclear export of actin: a novel mechanism regulating the subcellular localization of a major cytoskeletal protein. *EMBO J.* **17**, 1635-1641.

Wagner, K. R. (2002). Genetic diseases of muscle. *Neurol. Clin.* **20**, 645-678.